Heliyon 9 (2023) e16117

Contents lists available at ScienceDirect

Heliyon

journal homepage: www.cell.com/heliyon

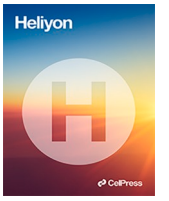

Research article

Integration of UHPLC/Q-OrbitrapMS-based metabolomics and activities evaluation to rapidly explore the anti-inflammatory components from lasianthus

Lele Zhang [a,1], Shaofei Song [a,1], Biying Chen [a], Rongrong Li [a], Liming Wang [a], Chenxi Wang [a], Lifeng Han [a,c], Zhifei Fu [a], Zhonglian Zhang [b,*], Qilong Wang [a,c,**], Heshui Yu [a,***]

[a] State Key Laboratory of Component-based Chinese Medicine, Tianjin Key Laboratory of TCM Chemistry and Analysis, Tianjin University of Traditional Chinese Medicine, 10 Poyanghu Road, Jinghai District, Tianjin 301617, PR China
[b] Yunnan Key Laboratory of Southern Medicine Utilization, Yunnan Branch of Institute of Medicinal Plant Development, Chinese Academy of Medical Sciences, Peking Union Medical College, Jinghong, 666100, China
[c] Haihe Laboratory of Modern Chinese Medicine, Tianjin, 301617, PR China

ARTICLE INFO

Keywords:
Lasianthus
Metabolomics
Mass defect filter
Anti-inflammatory
UHPLC/Q-Orbitrap-MS

ABSTRACT

Lasianthus, belonging to Rubiaceae, has been verified to improve clinical syndrome in immune diseases (e.g., hepatitis, nephritis, and rheumatoid arthritis). Both the anti-inflammatory function and chemical composition of Lasianthus vary considerably between different species but few studies focus. So essential it is to explore lasianthus and further search for anti-inflammatory substances. The target of this artical is to analyze the anti-inflammatory activity and chemical composition of lasianthus of different species. And the subsequent active compounds were explored. Primary, the anti-inflammatory activity among seven species of lasianthus (e.g., *L. fordii.*, *L. wallichii.*, *L. hookeri* C., *L. verticillatus.*, *L. sikkimensis.*, *L. appressihirtus., and L. hookeri* var) were evaluated by *vitro* experiments (RAW 264.7 cells). Next, UHPLC/Q-Orbitrap-MS-based metabolomics and the mass defect filter (MDF) algorithm were performed to explore metabolites. In addition, principal component analysis (PCA) was to screen out differential compounds in seven species. Finally, the correlation analysis between activities and composition to rapidly discover the active compounds (compounds were verified pharmacologically). Among the 7 species of lasianthus, the *L. fordii.* and *L. hookeri* C indicated the best anti-inflammatory activity. Untargeted metabolomics and MDF show 112 compounds, classified into six dominant types (e.g., flavonoids, phenolic acids, alkaloids, iridoids, coumarins, and anthraquinones). Furthermore, 33 differential metabolites were confirmed by PCA. Then according to correlation analysis and pharmacological validation, 7 compounds $IC_{50} < 100$ (e.g., scopoletin, asperulosidic acid, chlorogenic acid, ferulic acid, betaine, syringic acid, and emodin) were verified as anti-inflammatory compounds and conduct quantitative analysis. Metabolomics integrated with

* Corresponding author.
** Corresponding author. State Key Laboratory of Component-based Chinese Medicine, Tianjin Key Laboratory of TCM Chemistry and Analysis, Tianjin University of Traditional Chinese Medicine, 10 Poyanghu Road, Jinghai District, Tianjin 301617, PR China.
*** Corresponding author.
E-mail addresses: zzl0605@163.com (Z. Zhang), wangqilong_00@hotmail.com (Q. Wang), hs_yu08@163.com (H. Yu).
[1] Contributed to this work equally and share first authorship.

https://doi.org/10.1016/j.heliyon.2023.e16117
Received 25 March 2023; Received in revised form 21 April 2023; Accepted 6 May 2023
Available online 23 May 2023

activities evaluation might be a rapid and effective strategy to explore the active compounds from natural products.

1. Introduction

Lasianthus is a genus belonging to Rubiaceae, which includes about 180 species all over the world. According to the literature, there are 34 species, 4 subspecies, and 10 varieties in China [1,2]. The chemical composition of the lasianthus is quite complex, including quinones, terpenes, phenylpropanoids, flavonoids, steroids, and volatile oils [3–7]. The plants of lasianthus are famous folk medicine in the southwest of China and are widely used in the treatment of hepatitis, nephritis, rheumatic arthralgia, and lumbar muscle strain [8,9]. Although the resource of lasianthus is rich in China, and it demonstrates a broad prospective development in new drug discovery, there are few studies on its chemical constituents and modern pharmacological research up to now.

Metabolomics is an important tool for the research of systematical biology, which aims to study small-molecule metabolites and their changes in plants, animals, as well as single cells [10–12]. High-performance liquid chromatography combined with mass spectrometry (LC-MS) has gradually become one of the most universal tools in metabolomics research due to its outstanding sensitivity, high precision, and good reproducibility [13,14]. Currently, a lot of LC-MS-based untargeted metabolomics studies are performed for comprehensive evaluation of traditional Chinese medicine (TCM) and classification of different plant species or habitats [15–19]. Data-dependent acquisition (DDA) is usually used in MS/MS scans to assist in the identification of metabolites. DDA strategy preferentially selects relatively stronger signals for further fragmentation, it is difficult to acquire MS/MS ions of lower abundance metabolites. Therefore, selective DDA based on the precursor ions list can help to obtain more fragment ions.

Mass defect is the difference between the exact mass and nominal mass, which depends on the molecular composition of the compound. The mass defect filter (MDF) is setting the mass tolerance and mass defect tolerance based on high-resolution mass spectrometry data and then excludes ions that fall out of the expected range to obtain the mass spectrum data [20]. The inclusive scope of the MDF model is that the fractional part and the integer part of the m/z values would show a fixed range with the shift of the molecular weight for similar compounds. The strategy could eliminate background interference and reduce the false positive rate in the generation of MS/MS fragments effectively [21]. In general, a variety of structural types of secondary metabolites of Traditional Chinese medicine, and the same type of metabolites often share a common biosynthetic pathway. Therefore, the same type of secondary metabolites generally has a similar parent nuclear, combined with various substituent groups, including hydroxyl, methyl, methoxy, different sugar groups, etc. After fully considering the structural types of target compounds and the changes of potential substituents, the appropriate mass defect limit was selected and the constructed mass defect filtering window was applied to the data, which could automatically filter out interfering ions and realize the rapid identification of various natural products in traditional Chinese medicine [22]. In recent years, multiple MDF [23], linear gradient MDF [24], stepwise MDF [25], multi-point screening MDF [26], grid MDF, discrete MDF [27], deep learning MDF, Kendrick MDF, and other modified MDF techniques have been developed, which provide more methods for the study of composition characterization of the complex traditional Chinese medicine.

In this paper, the anti-inflammatory activities of seven species of lasianthus were evaluated. Furthermore, we proposed an LC-MS-based untargeted metabolomics combined with an MDF algorithm to investigate metabolites of lasianthus. Combined with PCA, different metabolites were selected from different varieties of lasianthus. Based on the correlation analysis between components and activities, the potential anti-inflammatory compounds were quickly screened out. Finally, the anti-inflammatory activities of the explored compounds were verified. Our work could not only be used to discover the differential compounds among different species of lasianthus, but also could help to strengthen quality control and promote new drug development from traditional herbal medicine.

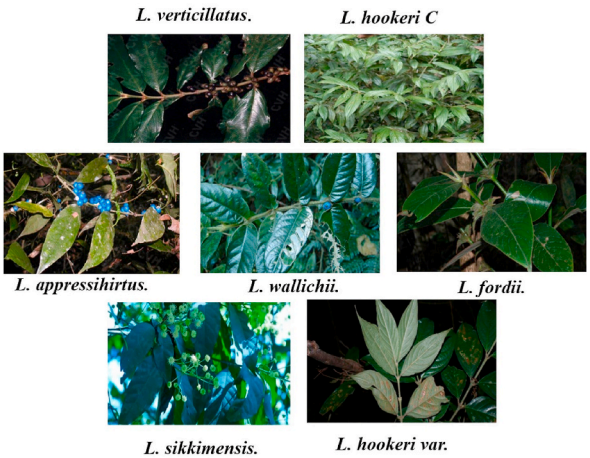

Fig. 1. The seven species of lasianthus.

2. Materials and methods

2.1. Plant collection

These plants were identified as *L. fordii.* (MZ); *L. wallichii.* (XJ); *L. hookeri* C. (HK); *L. verticillatus.* (XM); *L. sikkimensis.* (XIJ); *L. appressihirtus.* (XN) and *L. hookeri* var. (JM). A total of the 77 batches were authenticated by Professor Zhonglian Zhang from Yunnan Branch of Institute of Medicinal Plant Development, Chinese Academy of Medical Sciences. The species of different varieties of lasianthus were shown in Fig. 1. The habitat of different varieties of lasianthus were shown in Table S1.

2.2. Materials and reagents

HPLC-grade acetonitrile and methanol were obtained from Fisher Scientific (Fair Lawn, NJ, USA). While an HPLC-grade acetic acid was purchased from ACS (Wilmington, DE, USA; FA). Ultra-pure water was prepared by a Milli-Q water purification system (Millipore, Bedford, MA, USA). All other reagents were of analytical grade. The reference standards, including betaine, salicylic acid, vanillic acid, kaempferol, ferulic acid, formononetin, apigenin, asperuloside, asperulosidic acid, chlorogenic acid, scopoletin, berberine, syringic acid, 3-hydroxyflavone, asiatic acid, emodin, vanillin, citric acid, palmitic acid, 4-methoxycinnamic acid, 2-hydroxycinnamic acid, caffeic acid, malic acid, quinic acid and salicylic acid were purchased from Shanghai Yuanye Biotech. Co., Ltd (Shanghai, China).

RAW 264.7 cells were obtained from Procell Life Science&Technology Co., Ltd (Wuhan, China). Dulbecco's Modified Eagle's Medium (DMEM) and penicillin/streptomycin were purchased from Gibco (Grand Island, NY, USA). Fetal bovine serum (FBS), lipopolysaccharide (LPS), and dimethylsulfoxide (DMSO) were obtained from Sigma (St. Louis, MO, USA). Nitric Oxide Assay kit was purchased from Beyotime Biotechnology (Shanghai, China).

2.3. Standard solutions and sample preparation

77 batches of lasianthus were dried in the constant temperature oven for five days and then ground into powder by grinder (pass through sieve No.3). The 2 g of powder of different lasianthus samples was accurately weighed, and 40 mL of ethanol: water (30:70, *v/v*) was added. After ultrasonic extraction for 30 min, the extracts were centrifuged (Eppendorf 5424 R, Barkhausenweg 1, Hamburg, Germany) at 13,200 *g* for 10 min. Then, 5 μL of supernatant was injected for UHPLC/Q-Orbitrap MS analysis. To ensure the stability and accuracy of the measurement throughout the analysis, the quality control (QC) sample was prepared by taking all samples of lasianthus together, then the same QC samples were injected periodically after five samples injections, and the data obtained were used to evaluate the quality of the obtained dataset.

The stock solutions of scopoletin, asperulosidic acid, betaine, syringic acid, emodin, chlorogenic acid, salicylic acid and ferulic acid were accurately weighed to 1 mg respectively, into 1.5 mL centrifuge tubes and add methanol. A standard solution of the mixtures was prepared in concentration ranging from 25 to 4000 ng/mL by diluting stock solutions and refrigerated at 4 °C until use.

2.4. Evaluation of anti-inflammatory activities of all batches of lasianthus

RAW 264.7 cells were cultured in DMEM containing 10% FBS, and 100 U/mL penicillin at 37 °C for 24 h in a constant temperature incubator with 5% CO_2. Cells were seeded on a 96-well plate with a density of 1×10^5 cells/mL. The cells were treated with the extract (100 μg/mL) for 1 h, then stimulated with LPS (1 μg/mL) for 18 h. The concentration of Nitric oxide (NO) in the culture medium was measured by using the Greiss reagent kit. In brief, the supernatant of culture medium (50 μL) was mixed with 100 μL of Griess reagent for 3 min at 25 °C, and the absorbance values were measured at 540 nm on an enzyme-linked immunosorbent assay. Dexamethasone (10 μmol/L) was used as the positive drug.

2.5. Analytical chemical composition of lasianthus

2.5.1. UHPLC/Q-Orbitrap MS analysis

Untargeted metabolomics was performed with an Ultimate 3000 ultra-high performance liquid chromatography combined with a Q-Orbitrap MS system (Thermo Fisher Scientific, San Jose, CA, USA). Chromatographic separation was achieved on a Waters HSS T_3 column (2.1 × 100 mm, 1.7 μm). The temperature for the column oven and automatic sampler was set as 30 °C and 4 °C, respectively. The mobile phase consisted of 0.1% acetic acid in water (A) and acetonitrile (B) with a flow rate of 0.3 mL/min. Gradient elution was performed as follows: 0–5 min, 0–100% B; 5–7 min, 100%–100% B; 7–8 min, 100%–5% B; 8–10 min, 5% B. The injection volume was 5 μL.

High-accuracy MS data were obtained on a Q-Exactive™ hybrid quadrupole-Orbitrap mass spectrometer (Thermo Fisher Scientific, San Jose, CA, USA). The heated electrospray ionization (HESI) source parameters were set as follows: spray voltage, 3.0 kV for -ESI and 3.5 kV for + ESI; sheath gas pressure, 35 psi; auxiliary gas pressure, 10 arb (N_2, 99.9% purity); capillary temperature, 320 °C; and auxiliary gas heater temperature, 350 °C. The scan range of full MS was *m/z* 100–1,500, and the resolution was set as 70,000. A data-dependent scan (dd-MS^2) was applied to acquire high-quality MS/MS data. The MDF model was utilized to build a list of precursor ions, and the precursor ions list was used to get MS/MS data preferentially. The parameters of MS/MS were set as follows: resolution, 17,500; isolation window, 4 Da. The normalized collision energy (NCE) was used and set as 20/40/60 V. All the data were recorded and processed by Thermo Scientific Xcalibur 4.0 software (Thermo Fisher Scientific).

2.5.2. MDF algorithm was established to assist identification

The MDF algorithm was developed to achieve high specificity in the screening of targeted components from both negative and positive ions modes in a full-scan spectrum of lasianthus. In essence, it was constructed by the *m/z* values of the compounds in lasianthus, however, few studies on the chemical constituents of lasianthus were done. Therefore, a total of 80 compounds were identified from the QC sample by using Compound Discoverer™ software (Thermo Scientific, San Jose, CA, USA) as a database initially. The integer and decimal parts of *m/z* values from 80 compounds were located at the x-axis and y-axis to establish the scatter plot, and six boundaries were plotted by using the six outermost compounds. The corresponding "IF'' function could be calculated for each boundary, and the mass defect tolerance was set as ± 0.01 Da. The "IF" function was utilized to screen target ions from the full scan MS data. The MS data were recorded by UHPLC/Q-Orbitrap MS and processed by SIEVE software (Thermo Fisher Scientific) to yield a list containing the *m/z* values of the picked ions (metabolic features). Finally, the precursor ions list was constructed by target ions for the obtaining of further fragmentation.

2.5.3. Differential metabolites were analyzed

Compound Discoverer 3.0 was used for processing raw datasets of all batches of lasianthus, mainly including peak extraction, peak alignment, peak matching, and metabolite identification. The peak lists were further processed for area normalization, principal component analysis (PCA), and orthogonal partial least squares discriminant analysis (OPLS-DA) by SIMCA-P 14.1. All variables were Pareto scaled (Par) before analysis. Metabolites satisfying $VIP > 1$ and $p < 0.01$ (Student's t-test) were selected as differential metabolites. Metlin, PubChem, *m/z* Cloud (Thermo), and PCDL database (Agilent) were used for putative identification of significantly differential compounds.

2.6. Correlation analysis

Currently, correlation analysis has been widely used to relate chemical constituents with biochemical indices [28,29]. To further determine whether those differential chemical compounds are responsible for the anti-inflammatory activities, correlation analysis was carried out. Correlation analysis is done by calculating the correlation coefficient between samples, and gradually clustering the samples with the greatest correlation together until all the samples are grouped into one category [30]. The heatmap was utilized to visualize the changes in the content of the compounds in the different samples. Based on the results of the activities evaluation, several compounds were screened to be positively correlated with activity. To avoid false positive results, the potential active compounds were further verified (the method is described in 2.4).

2.7. Quantitative analysis of main compounds

2.7.1. UHPLC–MS instrument conditions

Ultrahigh performance liquid chromatography (UHPLC) analysis was performed using Shimadzu LC-30AD system (Shimadzu, Kyoto, Japan). Separation was fulfilled by using ACQUITY UPLC BEH C_{18} column (Waters, 1.7 μm, 2.1 × 100 mm). The mobile phase was composed of 0.1% Formic acid-water (A) and acetonitrile (B). The gradient elution was set as follows: 0−6 min, 5–95% B; 6−7 min, 95−95% B; 7−8 min, 95−95% B; 8−9 min, 5−5% B. The flow rate was set as 0.3 mL/min, and the injection volume was 2 μL.

Mass spectrometry was performed with a triple quadrupole linear ion trap mass spectrometer (QTRAP 6500$^+$) (AB SCIEX, Framingham, MA, USA) equipped with an ESI source. The general MS parameters were set as follows: gas temperature, 400 °C; ion spray voltage, 5500 V; GS1 and GS2, both 50 psi; and CUR, 35 psi. The mass spectrum conditions of the eight main components are shown in Table 1.

2.7.2. Validation of the quantitative analysis

The solution containing 8 reference compounds was prepared and diluted to six-point calibration levels for the construction of calibration curves. Each concentration of the mixed standard solution was injected in triplicate. Calibration curves were established by plotting the peak area versus concentration of each analyte. The limitation of detection (LOD) and quantification (LOQ) for each standard were defined at signal-to-noise ratio (S/N) of 3 and 10, respectively. Intra-day variations were utilized to assess the precision of the method and was determined by analyzing six replicates of sample within 1 day. Stability is used to assess whether the instrument is stable, the same solution was taken for analysis at time points 0, 1, 2, 4, 6, 8, 10, 12 and 24 h, respectively. To confirm the

Table 1
MS parameters of the target analytes.

Compounds	RT (min)	Precursor Ion (*m/z*)	Product Ion (*m/z*)	Cone voltage (V)	Collision Energy (V)
asperulosidic acid	5.3	432.12	119.1	23	40.93
syringic acid	3.23	198.05	78	35.88	14.16
emodin	6.33	270.05	225	34.27	144.08
salicylic acid	3.48	138.03	92.9	21	29.68
ferulic acid	2.53	194.05	78.8	26	105
betaine	0.86	385.30	58.1	33.63	83.93
scopoletin	3.46	353.27	103.9	32.98	36
chlorogenic acid	2.93	354.09	191.1	19.08	24

repeatability, six replicates of the same sample were extracted and analyzed. Variations were expressed by relative standard deviation (RSD) in all three tests above.

2.8. Data processing

Compound Discoverer 3.0 (Thermo Fisher Scientific, San Jose, CA, USA) was used for processing raw datasets. Principal component analysis (PCA) and orthogonal partial least squares discriminant analysis (OPLS-DA) by SIMCA-P 14.1 (Umetrics AB, Umea, Sweden). In addition, MultiExperiment Viewer software (MeV, version 4.9.0, TM4 Microarray Software Suite, Boston, MA) was used to generate heatmaps, and GraphPad Prism 9 (GraphPad) was used to generate column charts. One-way ANOVA was used to compare differences between groups. $P < 0.01$ was considered a statistically significant difference.

3. Results and discussion

3.1. Optimize the parameters of extraction and analysis

The extraction method was compared, and ultrasonic extraction was chosen at last for its high efficiency and convenient operation. The extraction solvent and time were also optimized, respectively. According to the recovery, intensity, and the number of peaks, methanol-water (30:70, *v/v*) and 30 min was selected as the optimal condition. The chromatographic conditions were optimized with different chromatographic columns, the type and concentration of the additive in the mobile phase, and the column temperature. According to the resolution of the chromatographic peaks, the HSS T3 column and 0.01% acetic acid in water were selected as analytical conditions, and the best column temperature for LC-MS analysis was 30 °C. The NCE of MS conditions was optimized. According to the intensity and quantity of MS/MS fragments of scoparone, 3-hydroxyflavone, asperuloside, emodin, 20/40/60 V was selected as the acceptable parameter. The above results were shown in Supplementary Figs. S7–S13.

3.2. Results of the anti-inflammatory activities

Excessive NO production is involved in the pathogenesis of inflammatory diseases. The anti-inflammatory activities of the different species of lasianthus were evaluated by detecting the inhibition rate of NO in RAW 264.7 macrophages. The inhibition rate of NO in the model group was set as 100%, and the other samples were expressed as a percentage of the standard value. Each sample preparation in three for testing. The results were shown in Fig. 2A, compared with the control group, the model group was stimulated with LPS (1 μg/mL), which resulted in a significant increase in NO release (100%). Compared with the model group, the whole experimental groups have significant inhibitory effects on NO release, NO (%) of all groups was less than 100%. In addition, MZ and HK showed a better inhibitory effect on the production of NO, and NO (%) was significantly lower than other species in Fig. 2A. In Fig. 2B, although samples are from the same origin, there are also differences in conditions, resulting in different chemical compositions and anti-inflammatory activity of batches of MZ and HK. Further analysis of the chemical composition, we found that more polyphenolic compounds (asperulosidic acid, chlorogenic acid, ferulic acid, salicylic acid, syringic acid, Asiatic acid, vanillic acid, abscisic acid, etc.) and flavonoids (apigenin, kaempferol, rubiadin, formononetin, etc.) were scattered in different batches of MZ and HK. These compounds have been reported to have anti-inflammatory activity. Furthermore, MZ-4, MZ-5, HK-3, HK-5, and HK-6 have significant anti-inflammatory activities, which were even better than that of dexamethasone as shown in Fig. 2B. The inhibition ratio of all lasianthus on NO production in RAW 264.7 cells is shown in Table 2.

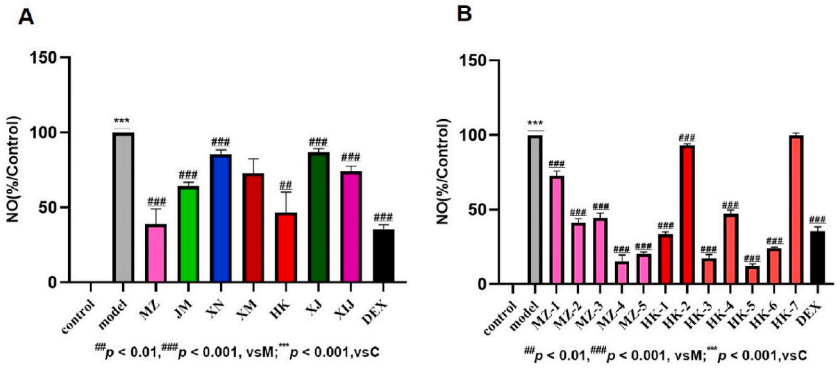

Fig. 2. Anti-inflammatory activities of different species of lasianthus (A) and different samples (B) (***$p < 0.001$ versus control group; $^{\#\#}p < 0.01$, $^{\#\#\#}p < 0.001$ versus model group).

3.3. Composition analysis of lasianthus

3.3.1. Identification of compounds based-MDF

To elucidate the chemical constituents of seven species of lasianthus as much as possible, the UHPLC/Q-Orbitrap-MS-based untargeted metabolomics combined with the MDF algorithm was utilized in our strategy. Firstly, QC samples were analyzed for profiling the chemical composition, and the typical base peak chromatogram (BPC) of positive ion mode and negative ion mode was shown in Fig. 3A and B. Metabolites assignment was based on the molecular elements composition, retention time, accurate MS and MS/MS data by comparing with reference compounds, kinds of literature, and online databases. A total of 53 compounds in the negative mode and 27 compounds in the positive mode were detected, which were used as the database of the MDF algorithm. Secondly, the MDF window was constructed in GraphPad Prism 9.0 software to selectively screen out more compounds. As shown in Fig. 4A, a polygon MDF window was established, and the correlation equations of all the red dots were calculated, which were called "IF'' equations as follow:

$y \leq 2.7928–0.0052x+0.01$ $(471 \leq x \leq 515)$;

$y \geq -0.0907 + 0.0004x-0.01$ $(283 \leq x \leq 515)$;

$y \geq -0.0108 + 0.0001x-0.01$ $(115 \leq x \leq 283)$;

$y \leq -7.8186 + 0.068x+0.01$ $(115 \leq x \leq 116)$;

$y \leq -0.0994 + 0.0015x+0.01$ $(116 \leq x \leq 282)$;

$y \leq 0.2698 + 0.0002x+0.01$ $(282 \leq x \leq 471)$.

As shown in Fig. 4B, the blue dots refer to the full scan MS data (mass range: *m/z* 100–1500), then "IF'' equations were used to exclude false positive ions. 533 potential ions (red dots) were obtained in the established inclusion list. Based on the established UHPLC/Q-Orbitrap-MS analysis method, a total of 66 compounds in the negative mode and 46 compounds in the positive mode were detected. Among them, 22 compounds were unambiguously identified by comparison with reference standards. Besides, 90 components were subjected to further analysis and validation. Supplementary information was shown in Table S1. They mainly included flavonoids, phenolic acids, alkaloids, iridoids, coumarins, anthraquinones, and other types. We further took different types of compounds as examples to demonstrate analysis of the chemical composition. Supplementary information of other fragmentation behaviors was shown in Figs. S14–17.

Comp. 14. Molecular ions of $[M-H]^-$at *m/z* 431.1194 ($C_{18}H_{23}O_{12}$) were observed in the MS^1 spectrum. The fragment ion *m/z* 269.0674 ($[M\text{-}H\text{-}Glc]^-$) was formed by $[M-H]^-$removing a molecule of glucose, and then losing H_2O to produce fragment ion of *m/z* 251.0563 ($[M\text{-}H\text{-}Glc\text{-}H_2O]^-$). The fragment ion *m/z* 207.0645 ($[M\text{-}H\text{-}Glc–H_2O–CO_2]^-$), *m/z* 165.0548 ($[M\text{-}H\text{-}Glc–H_2O–CO_2–C_2H_2O$]

Table 2
Inhibitory ratio of 77 batches of lasianthus on NO production in RAW 264.7 cells.

Batches	NO (%)	Batches	NO (%)	Batches	NO (%)
MZ-1	72.64 ± 5.47	XN-1	84.63 ± 8.65	XIJ-1	66.31 ± 3.84
MZ-2	41.34 ± 4.52	XN-2	93.59 ± 6.2	XIJ-2	61.69 ± 3.84
MZ-3	44.59 ± 5.33	XN-3	103.46 ± 11.75	XIJ-3	96.07 ± 3.83
MZ-4	15.31 ± 7.35	XN-4	73.2 ± 5.03	XIJ-4	96.15 ± 4.05
MZ-5	20.3 ± 2.27	XN-5	79.75 ± 6.26	XIJ-5	63.8 ± 3.04
JM-1	57.48 ± 5.01	XN-6	86.23 ± 7.04	XIJ-6	60.4 ± 4.71
JM-2	57.22 ± 2.77	XN-7	75.53 ± 4.37	XIJ-7	58.45 ± 6.09
JM-3	68.08 ± 2.79	XN-8	75.6 ± 4.75	XIJ-8	67.95 ± 2.12
JM-4	57.24 ± 1.98	XN-9	78.08 ± 3.73	XIJ-9	81.25 ± 6.86
JM-5	81.71 ± 7.91	XN-10	95.15 ± 5.1	XIJ-10	52.61 ± 3.62
JM-6	73.18 ± 2.38	XN-11	94.39 ± 4.05	XIJ-11	87.45 ± 5.65
JM-7	63.93 ± 4.86	XM-1	57.43 ± 2.33	XIJ-12	54.95 ± 1.73
JM-8	58.65 ± 0.15	XM-2	65.23 ± 3.83	XIJ-13	83.85 ± 3.64
JM-9	64.47 ± 0.88	XM-3	83.11 ± 4.45	XIJ-14	88.84 ± 7.56
JM-10	60.72 ± 2.29	XM-4	105.05 ± 3.15	XIJ-15	58.38 ± 5.36
HK-1	33.54 ± 2.68	XM-5	53.99 ± 1.56	XIJ-16	86.18 ± 2.66
HK-2	93.16 ± 1.5	XJ-1	94.21 ± 2.49	XIJ-17	64.23 ± 6.32
HK-3	17.39 ± 4.21	XJ-2	75.4 ± 1.58	XIJ-18	83.38 ± 4.13
HK-4	47.17 ± 4.33	XJ-3	92.91 ± 0.14	XIJ-19	94.71 ± 7.89
HK-5	12.17 ± 2.36	XJ-4	82.32 ± 3.08	XJ-8	76.44 ± 5.8
HK-6	24.23 ± 1.03	XJ-5	82.32 ± 3.08	XJ-9	97.22 ± 5.48
HK-7	99.83 ± 2.53	XJ-6	80.92 ± 1.64	XJ-10	73.97 ± 3.45
XJ-11	95.43 ± 1.21	XJ-7	115.24 ± 2.55	XJ-17	72.02 ± 1.75
XJ-12	94.45 ± 3.54	XJ-14	81.65 ± 0.79	XJ-18	83.38 ± 1.46
XJ-13	89.83 ± 3.16	XJ-15	96.82 ± 1.45	XJ-19	89.79 ± 3.07
–	–	XJ-16	83.75 ± 0.61	XJ-20	79.09 ± 0.25

Data were present as the mean ± SD ($n = 3$).

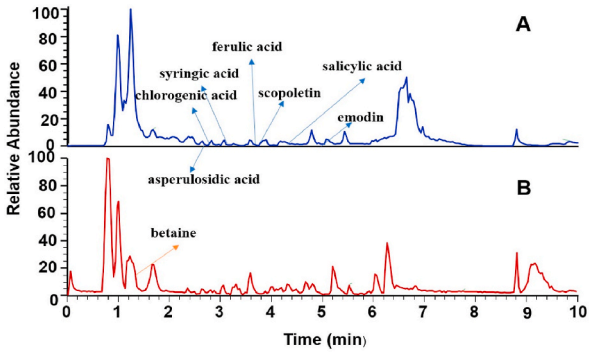

Fig. 3. The base peak chromatography in negative(A) and positive(B) ion mode of QC sample; Pick out of eight active compounds are shown in this figure.

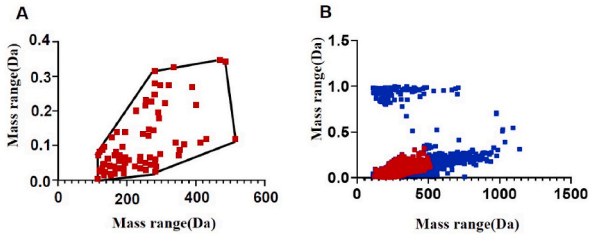

Fig. 4. The MDF model (A); The blue area refers to the full scan MS data and the red area refers to the data filtered by the MDF (B). (For interpretation of the references to colour in this figure legend, the reader is referred to the Web version of this article.)

$^{-}$) and *m/z* 147.0444 ([M-H-Glc–H_2O–CO_2–C_2H_2O–H_2O] $^{-}$) were generated by eliminating CO_2, C_2H_2O and H_2O from the *m/z* 251.0563 in succession. Ultimately, compound **14** and compound **5** were tentatively identified as asperulosidic acid and asperuloside. The proposed fragmentation pathway was in accordance with the previous reports [31]. The fragmentation behavior of asperulosidic acid was illustrated in Fig. 5A.

Comp. 52. Molecular ions of [M − H]−at *m/z* 267.0666 ($C_{16}H_{12}O_4$) were observed in the MS^1 spectrum. The fragment ion *m/z* 252.0462 ([M-H-CH_3] $^{-}$) and *m/z* 251.0352 ([M-H-O] $^{-}$) was formed by [M − H]−removing CH_3 and an O atom, and then losing 2CO to produce fragment ions of *m/z* 223.0408 ([M-H-O-CO] $^{-}$) and *m/z* 195.0448 ([M-H-O–CO–CO] $^{-}$) consecutively. The fragment ion *m/z* 208.0576 was formed by eliminating CH_3 from the *m/z* 223.0408 ([M-H-O–CO–CO-CH_3] $^{-}$). Ultimately, compounds **2**, **7**, **39**, **52,** and **91** were tentatively identified as 3-hydroxy flavone, genistein, kaempferol, formononetin, and apigenin. The proposed fragmentation pathway was in accordance with the previous reports [32]. The fragmentation behavior of formononetin was illustrated in Fig. 5B.

3.3.2. Metabolomics profiling analysis

MZ, XJ, XIJ, XN, XM, and JM were different species of lasianthus, which have similar chemical composition, however the contents of those chemicals were different resulting in different anti-inflammatory activities. The purpose of the study is to find compounds with different content and discover the potential active substances rapidly. A total of 80 samples were analyzed by the optimized UHPLC/Q-Orbitrap-MS method. Raw data were pretreated using CD software, a peak list was obtained further for multivariate statistical analysis. In the unsupervised PCA score plot (Fig. 6A), seven species of lasianthus could be well separated. And a tight clustering of the QC group indicated that the LC-MS system is stable during the analysis. Subsequently, we selected samples of MZ and other species for further OPLS-DA analysis respectively, because all samples in MZ had significant anti-inflammatory activity ($p < 0.001$), and more different compounds could be found. OPLS-DA (Fig. 6B.) was utilized to classify different groups and further probe differential components ($R^2X = 0.68$, $R^2Y = 1$, $Q^2 = 0.984$). To identify the significantly altered metabolites, the VIP value ($VIP > 1$) from multivariate data analysis and the p-value ($p < 0.01$) of the *t*-test between the seven species were chosen as the criteria for markers discovery. In addition, hotelling's T_2 verification (Fig. 6C.) and 200 permutation tests (Fig. 6D.) were carried out on the OPLS-DA model, and the results showed that the model was not overfitted and had good prediction ability. A total of 33 variables were screened out, 15 differential compounds were identified between MZ and XN, and 13 differential compounds were screened between MZ and HK. 14 differential compounds between MZ and JM, 20 differential compounds between MZ and XIJ, 11 differential compounds between MZ and XJ, and 9 differential compounds between MZ and XM were also were screened out, respectively. OPLS-DA models of different species of lasianthus were shown in Supplementary Fig. S18.

The specific compounds and ROC analysis were shown in Supplementary Table S3 and Figs. S1–S6.

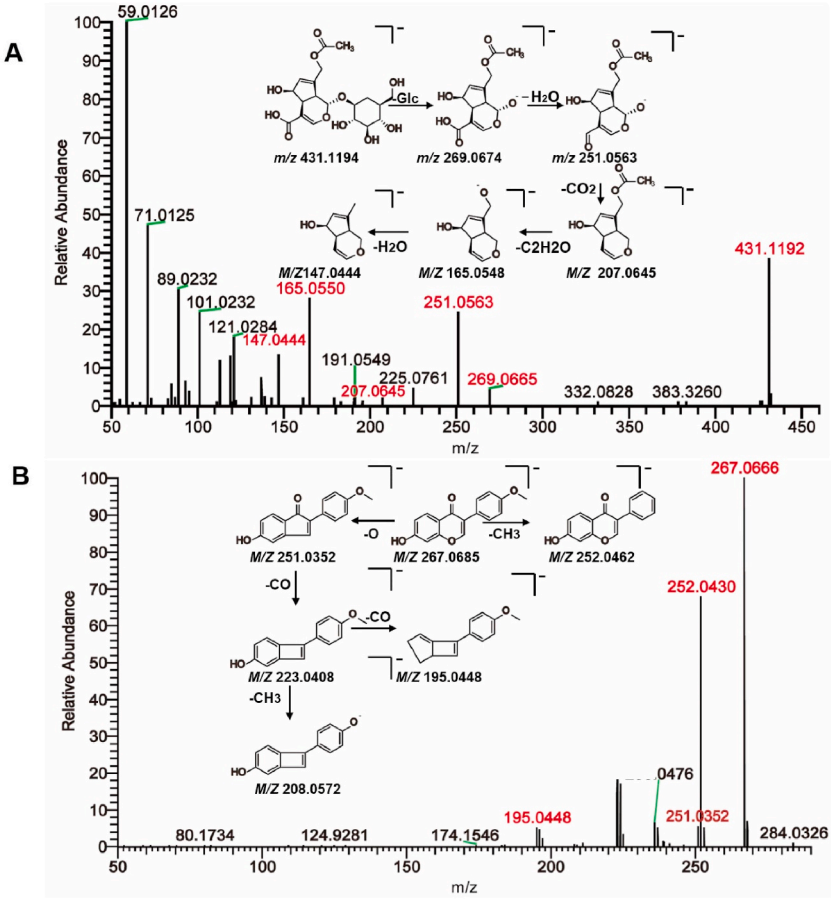

Fig. 5. The fragmentation behavior of asperulosidic acid (A) and formononetin (B).

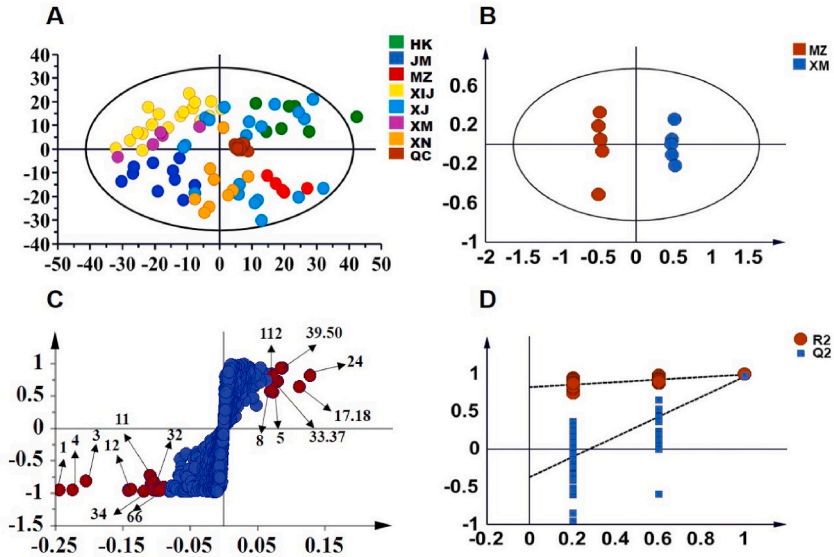

Fig. 6. Multivariate statistical analysis of different species of lasianthus. (A: PCA scores plots; B: OPLS-DA scores plots; C: S-plot; D: 200 permutation tests).

3.4. Searching for active substances with correlation analysis

According to the anti-inflammatory activities evaluation *in vitro*, MZ and HK of lasianthus exhibited significant anti-inflammatory activities. Furthermore, MZ-4, MZ-5, HK-3, HK-5, and HK-6 showed relatively higher anti-inflammatory activities than the others, which were much better than dexamethasone. To rapidly search for potential active substances in the five active samples more comprehensively and intuitively, correlation analysis was used to elucidate the results. As shown in Fig. 7, the red area refers to compounds with high content, mainly distributed at both ends; the blue area refers to compounds with less content, mostly focused on the middle region. Combine with the active substances of anti-inflammation reported in the literature [33–39], eight compounds in the red area were screened out as the potential anti-inflammatory active components, including scopoletin, asperulosidic acid, chlorogenic acid, ferulic acid, betaine, salicylic acid, syringic acid, and emodin.

3.5. Pharmacological validation

The anti-inflammatory activities of the eight compounds were verified. As shown in Table 3, scopoletin, asperulosidic acid, betaine, syringic acid, and emodin exhibited significant inhibition of NO production with an inhibitory concentration causes 50%inhibition (IC_{50}) value of 17.36 μmol/L, 28.49 μmol/L, 21.88 μmol/L, 19.43 μmol/L, and 26.77 μmol/L. Compared with other compounds, chlorogenic acid exhibited extremely significant inhibition of NO production with an IC_{50} value of 2.57 μmol/L. A moderate inhibitory effect was observed for ferulic acid, with an IC_{50} value of 60.36 μmol/L. Salicylic acid displayed weaker inhibitory effects with IC_{50} values > 100 μmol/L.

3.6. The results of quantitative analysis

3.6.1. Method validation of the quantitative analysis

The calibration curves, linear ranges, LOD and LOQ, and of 8 analytes were performed using the Q-TRAP-6500$^+$. Correlation coefficient values ($r^2 > 0.999$) indicated good correlations between standards concentrations and their peak areas. The ranges of LOD and LOQ for all the analytes were from 0.01 to 0.03 ng/mL, and 0.02 to 0.08 ng/mL, respectively. The intra-day present as (RSD) was between 0.78% and 4.84% of the 8 compounds. The stability variations (RSD) of the 8 analytes were in the range from 0.74 to 4.45%. The repeatability variations (RSD) of the 8 analytes were between 0.95% and 4.01%. Therefore, the results demonstrated that the method was sensitive, precise, and accurate. Detailed data are shown in Table 4 and Table 5.

3.6.2. Quantitative determination of MZ and HK

A total of 10.0 mg of lasianthus powder was obtained and 3 samples were obtained in parallel in each batch. The contents of 8 investigated compounds were summarized in Table 6. It was recognized that the contents of each compound varied in different species of lasianthus, even in different batches from the same species. For example, chlorogenic acid was abundant in the batches of MZ-4, HK-1, HK-2, HK-3 and HK-4, but lower in the batches of MZ-1, MZ-2, and MZ-5. Moreover, the content of chlorogenic acid in MZ-4 is much higher than MZ-1. According to Table 6 and it is shown that the contents of betaine, emodin, scopoletin, asperulosidic acid and chlorogenic acid were the main active substances in the MZ and HK with high content.

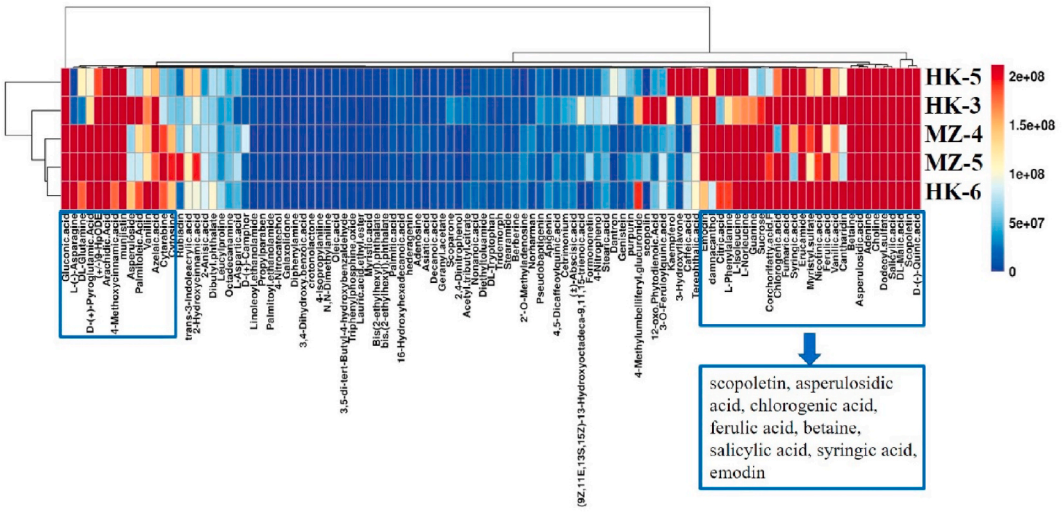

Fig. 7. Correlation analysis of compounds in MZ-4, MZ-5, HK-3, HK-5, and HK-6.

Table 3
Inhibitory activities of different compounds on NO production in RAW 264.7 Macrophage cells.

Compounds	NO IC_{50}(μmol/L)[a]
Chlorogenic acid	2.57 ± 0.7
Scopoletin	17.36 ± 3.1
Syringic acid	19.43 ± 5
Betaine	21.88 ± 9.7
Emodin	26.77 ± 40.8
Asperulosidic acid	28.49 ± 14
Ferulic acid	60.36 ± 24.4
Salicylic acid	>100

[a] Data were present as the mean ± SD ($n = 3$).

Table 4
Summary of calibration curves, linear range, LOD and LOQ for 8 compounds.

Analyte	calibration curves	Linear range (ng/mL)	LOD (ng/mL)	LOQ (ng/mL)
asperulosidic acid	Y = 126.37X+71339	25–4000	0.02	0.05
syringic acid	Y = 75.3X+439	25–4000	0.01	0.03
emodin	Y = 684.18X+8699.8	25–4000	0.03	0.08
salicylic acid	Y = 248.9X + 4991	25–4000	0.02	0.07
ferulic acid	Y = 525.3X + 1305	25–4000	0.02	0.05
betaine	Y = 920.89X+51543	25–4000	0.02	0.05
scopoletin	Y = 316.99X+13147	25–4000	0.01	0.02
chlorogenic acid	Y = 279.6X+8972	25–4000	0.01	0.02

Table 5
Stability, Precisions and recoveries of 8 analytes.

Analyte	Precisions Intra-day (RSD, %)	Recoveries (RSD, %)	Stability (RSD, %)
asperulosidic acid	1.82	1.16	0.94
syringic acid	3.55	3.56	1.68
emodin	3.56	3.9	4.44
salicylic acid	3.39	4.01	4.45
ferulic acid	2.21	0.95	3.06
betaine	0.78	2.94	0.74
scopoletin	4.84	3.56	1.68
chlorogenic acid	3.51	3.97	3.94

4. Discussion

The lasianthus have abundant resources and a broad prospect of development, which is considered a significant folk medicine in China. Nevertheless, at present, few types of research have been conducted. To provide the foundation for clinical research and the new drug development of lasianthus, executing systematic research on chemical constituents and pharmacological activities is essential. In this paper, we utilized LC-MS-based untargeted metabolomics combined with the MDF algorithm to investigate the differential metabolites of seven species of lasianthus. Meanwhile, the anti-inflammatory activities of all samples were evaluated. Based on the correlation analysis between components and activities, the potential anti-inflammatory compounds were screened out. Finally, seven compounds of chlorogenic acid, ferulic acid, scopoletin, asperulosidic acid, betaine, syringic acid, and emodin were verified to exhibit significant inhibition of NO production.

The anti-inflammatory activities of these compounds have been reported. Scopoletin inhibited the activities of prostaglandin E_2 (PGE_2), tumor necrosis factor-alpha (TNF-α), and leukotriene C4 (LTC4) in excess and neutrophil infiltration [40], and suppressed the production of proinflammatory cytokines such as IL-1β and IL-6 [41]. Asperulosidic acid significantly decreased the production of NO, PGE2, TNF-α, and IL-6 in parallel with the inhibition of inducible nitric oxide synthase (iNOS), cyclooxygenase-2 (COX-2), TNF-α and IL-6 mRNA expression in LPS-induced RAW 264.7 cells, and suppressed the phosphorylation of the inhibitors of nuclear factor-kappaB alpha (NFκB-α), extracellular signal-regulated kinase (ERK) and c-Jun N-terminal kinase (JNK) [42,43]. Chlorogenic acid significantly inhibited the production of NO and the expression of COX-2 and iNOS, without any cytotoxicity, and attenuated proinflammatory cytokines and other inflammation-related markers. Additionally, the nuclear translocation of NFκB-α, endotoxin-induced adhesion of macrophages, and the expression level of ninjurin1 (Ninj1) were decreased by chlorogenic acid [44]. Ferulic acid significantly inhibited IL-6, IL-1, and TNF-α and increased IL-10 mRNA and protein expression. Betaine inhibited NFκB-α and inflammatory-related cytokines such as TNF-α, IL-6, iNOS, and COX-2 [45]. Emodin inhibited NO production and the protein and mRNA expression of inducible nitric iNOS and COX-2. Furthermore, the decrease in P-gp expression is caused by the decreased expression of COX-2 through

Table 6
Quantitative determination of MZ and HK.

	Betaine	Emodin	Scopoletin	asperulosidic acid	Syringic acid	Chlorogenic acid	Salicylic acid	Ferulic acid
MZ-1	2786.66 ± 262.08	593.41 ± 10.02	778.76 ± 9.96	630.59 ± 8.24	65.51 ± 0.79	33.98 ± 2.12	24.5 ± 3.76	0.92 ± 0.03
MZ-2	1282.53 ± 108.55	1284.93 ± 20.25	1076.23 ± 6.94	421.18 ± 12.69	113.66 ± 22.47	47.56 ± 5.84	9.96 ± 1.57	3.22 ± 1.07
MZ-3	2169.42 ± 11.07	1361.64 ± 163.02	1342.40 ± 171.88	258.44 ± 1.38	81.54 ± 0.27	380.93 ± 99.59	33.99 ± 2.37	11.83 ± 1.32
MZ-4	1937.97 ± 390.50	1143.141 ± 20.25	3905.06 ± 417.7	733.08 ± 44.97	293.78 ± 27.64	5083.74 ± 374.15	204.71 ± 7.0	1.69 ± 0.01
MZ-5	1630.19 ± 17.56	6313.68 ± 3.80	804.29 ± 44.35	173.17 ± 143.35	107.33 ± 8.25	57.92 ± 6.98	9.51 ± 0.65	2.92 ± 0.39
HK-1	3220.46 ± 43.46	575.97 ± 17.25	5319.04 ± 68.5	423.37 ± 27.15	194.44 ± 1.75	2288.86 ± 4.80	9.05 ± 4.64	7.08 ± 0.08
HK-2	1956.41 ± 167.08	590.15 ± 14.2	2264.86 ± 0.04	471.89 ± 32.34	257.08 ± 37	2594.83 ± 160.16	44.24 ± 4.92	10.07 ± 1.76
HK-3	2201.96 ± 19.42	604.33 ± 13.65	3990.91 ± 15.08	615.25 ± 10.38	189.88 ± 16.72	1312.26 ± 13.06	20.66 ± 8.21	6.86 ± 0.79
HK-4	2111.01 ± 37.45	554.70 ± 10.22	5641.15 ± 63.6	213.45 ± 2.47	224.74 ± 1.38	7193.67 ± 161.195	115.2 ± 83.37	8.53 ± 0.06
HK-5	3874.901 ± 2.13	1043.88 ± 100.06	1773.92 ± 12.23	489.47 ± 21.97	206.14 ± 18.19	406.91 ± 13.16	5.73 ± 5.81	7.64 ± 0.86
HK-6	1670.68 ± 6.004	701.46 ± 22.85	2876.01 ± 43.7	452.17 ± 21.5	268.96 ± 46.3	258.33 ± 3.96	41.06 ± 10.18	10.64 ± 2.21
HK-7	1083.10 ± 10.88	580.93 ± 27.27	1262.28 ± 20.11	289.90 ± 2.5	209.11 ± 28.87	322.44 ± 8.79	17.16 ± 4.13	7.78 ± 1.37

Note: The unit is (ng/10 mg).

the MAPK/AP-1 pathway [46]. In this paper, the compounds with significant anti-inflammatory activities were screened out and verified.

In summary, the present study of the seven species of lasianthus showed an effective strategy to rapidly discover active compounds by a combination of anti-inflammatory activities, plant metabolomics, and the MDF algorithm.

5. Conclusion

In this study, we evaluated and compared the anti-inflammatory activities of MZ, XJ, XIJ, XN, XM, and JM. A technique for MDF data processing after acquisition is proposed for assisting identification and utilizing metabolomics to analyze the differences of compounds in lasianthus. Based on the correlation analysis of activities and content in different species, the potential active substances were rapidly screened out. After pharmacological verification with pure compounds, the substance basis of anti-inflammatory was finally discovered and quantitative analysis of major compounds was also performed. In summary, results showed more compounds could be identified using the MDF algorithm, and correlation analysis could be a rapid and effective way to screen active compounds. The developed characterization strategy with high sensitivity, selectivity, and coverage could provide a valuable reference for the in-depth analysis of other complex components in herbal medicines.

CRediT authorship contribution statement

Lele Zhang, Shaofei Song: Performed the experiments, Analyzed and interpreted the data, Wrote the paper.
Biying Chen, Rongrong Li: Analyzed and interpreted the data, Wrote the paper.
Liming Wang, Chenxi Wang: Conceived and designed the experiments, Wrote the paper.
Lifeng Han, Zhifei Fu: Contributed reagents, materials, analysis tools, Conceived and designed the experiments, Wrote the paper.
Zhonglian Zhang, Qilong Wang, Heshui Yu: Conceived and designed the experiments, Wrote the paper.

Data availability

The data that support the findings of this study are available from the corresponding author upon reasonable request. Original material also available upon request.

Declaration of competing interest

A Funding Source Declaration contains a declaration of any funding or research grants (and their source) received in the course of study, research or assembly of the manuscript.

Acknowledgments

The research was funded by Science and Technology Program of Tianjin (No.22ZYJDSS00100); National Key R&D Program of China (2019YFC1712304, 2019YFC1712305); CAMS Innovation Fund for Medical Sciences (CIFMS) (2021-I2M-1–032).

Appendix A. Supplementary data

Supplementary data to this article can be found online at https://doi.org/10.1016/j.heliyon.2023.e16117.

References

[1] T. Napiroon, M. Poopath, S. Duangjai, et al., Lasianthus yalaensis (Rubiaceae), a new species from peninsular Thailand, Phytotaxa 364 (2018).
[2] M. Cai, H. Zhu, H. Wang, Pollen morphology of the genus Lasianthus (Rubiaceae) and related taxa from Asia, J. Systemat. Evol. 46 (2008) 62–72.
[3] G.A. Al-Hamoud, R.S. Orfali, S. Perveen, K. Mizuno, K. Matsunami, A.E. Lasianosides, New iridoid glucosides from the leaves of lasianthus verticillatus (Lour.) Merr. And their antioxidant activity, Molecules 24 (2019) 3995.
[4] G.A. Al-Hamoud, R.S. Orfali, Y. Takeda, S. Sugimoto, Y. Yamano, N.M. Al Musayeib, O.I. Fantoukh, M. Amina, H. Otsuka, K. Matsunami, F.-I. Lasianosides, A new iridoid and three new bis-iridoid glycosides from the leaves of lasianthus verticillatus (Lour.), Merr. Mol. 25 (2020) 1070.
[5] H.A. Teng, A. Jm, B. Jz, A. Yz, A. Hw, A. Hl, A. Bl, Three new Anthraquinones, one new Benzochromene and one new Furfural glycoside from Lasianthus acuminatissimus, Nat. Prod. Res. 33 (2019) 1916–1923.
[6] X. Liu, T. Li, Y. Liu, H. Liu, X. Chen, J. Ming, X. Lai, B. Li, Six new anthraquinone glycosides from Lasianthus acuminatissimus Merr, Nat. Prod. Res. 35 (2021) 2535–2543.
[7] N.K.T. Pham, T.D.H. Nguyen, T.M.C. Nguyen, G.D. Nguyen, C.D. Huynh, T.N. Vo, T.Q.T. Nguyen, T.H. Duong, V.S. Dang, B.L.C. Huynh, T.N.M. Tran, T. P. Nguyen, Lasibidoupins A and B, two new compounds from the stems of Lasianthus bidoupensis V.S. Dang & Naiki, Nat. Prod. Res. (2021) 1–7.
[8] X.U. Bin, Z.C. Xie, X.Q. Lin, The effect of Lasianthus fardii Hance on duck hepatitis B, Mod. Prev. Med. 37 (2010) 2710–2712.
[9] M.A. Tan, M.W.D. Lagamayo, G.J.D. Alejandro, S.S. A, An, Neuroblastoma SH-SY5Y cytotoxicity, anti-amyloidogenic activity and cyclooxygenase inhibition of Lasianthus trichophlebus (Rubiaceae), 3 Biotech 10 (2020) 152.
[10] B. Shrestha, Single-cell metabolomics by mass spectrometry, Methods Mol. Biol. 2064 (2020) 1–8.
[11] J.F. Liu, Y.H. Yang, Y. Wu, J.T. Yang, Untargeted metabolomic profiling of liver and serum in mouse during normal aging, Zhongguo yi xue ke xue yuan xue bao 43 (2021) 536–544.

[12] N. Carriot, B. Paix, S. Greff, B. Viguier, J.F. Briand, G. Culioli, Integration of LC/MS-based molecular networking and classical phytochemical approach allows in-depth annotation of the metabolome of non-model organisms - the case study of the brown seaweed Taonia atomaria, Talanta 225 (2021), 121925.
[13] Z. Liao, S. Zhang, W. Liu, B. Zou, L. Lin, M. Chen, D. Liu, M. Wang, L. Li, Y. Cai, Q. Liao, Z. Xie, LC-MS-based metabolomics analysis of Berberine treatment in ulcerative colitis rats, J. Chromatogr., B: Anal. Technol. Biomed. Life Sci. 1133 (2019), 121848.
[14] X. Dong, S. Yao, W. Wu, J. Cao, W. Ren, Gas explosion-induced acute blast lung injury assessment and biomarker identification by a LC-MS-based serum metabolomics analysis, Hum. Exp. Toxicol. 40 (2020) 608–621.
[15] A. Tawfike, Metabolomics analysis and biological investigation of three Malvaceae plant, Phytochem. Anal. 31 (2020) 204–214.
[16] Z. Han, M. Wen, H. Zhang, L. Zhang, X. Wan, C.T. Ho, LC-MS based metabolomics and sensory evaluation reveal the critical compounds of different grades of Huangshan Maofeng green tea, Food Chem. 374 (2022), 131796.
[17] Qi Che, Xueyan Lu, Xiaorui Guo, et al., Metabolomics characterization of two apocynaceae plants, catharanthus roseus and Vinca minor, using GC-MS and LC-MS methods in combination, Molecules 22 (2017) 997.
[18] M. He, Y. Zhou, How to identify "Material basis-Quality markers" more accurately in Chinese herbal medicines from modern chromatography-mass spectrometry data-sets: opportunities and challenges of chemometric tools, Chin. Herb. Med. 13 (1) (2020) 2–16.
[19] M.T. Zuo, Y.C. Liu, Z.L. Sun, et al., An integrated strategy toward comprehensive characterization and quantification of multiple components from herbal medicine: an application study in Gelsemium elegans, Chin. Herb. Med. 13 (1) (2020) 17–32.
[20] J.X. Tian, Y. Tian, L. Xu, et al., Characterisation and identification of dihydroindole-type alkaloids from processed semen strychni by high-performance liquid chromatography coupled with electrospray ionisation ion trap time-of-flight mass spectrometry, Phytochem. Anal. 25 (1) (2014) 36–44.
[21] T. Tan, C.J. Lai, S.L. Zeng, et al., Comprehensive profiling and characterization of quassinoids from the seeds of Brucea javanica via segment and exposure strategy coupled with modified mass defect filter, Anal. Bioanal. Chem. 408 (2) (2016) 527–533.
[22] H. Xu, H. Niu, B. He, et al., Comprehensive qualitative ingredient profiling of Chinese herbal formula Wu-Zhu-Yu decoction via a mass defect and fragment filtering approach using high resolution mass spectrometry, Molecules 21 (5) (2016) 664.
[23] H.Q. Pan, W.Z. Yang, Y.B. Zhang, et al., An integrated strategy for the systematic characterization and discovery of new indole alkaloids from Uncaria rhynchophylla by UHPLC/DAD/LTQ-Orbitrap-MS, Anal. Bioanal. Chem. 407 (20) (2015) 6057.
[24] G. Yan, H. Sun, W. Sun, et al., Rapid and global detection and characterization of aconitum alkaloids in Yin Chen Si Ni Tang, a traditional Chinese medical formula, by ultra performance liquid chromatography-high resolution mass spectrometry and automated data analysis, J. Pharm. Biomed. Anal. 53 (3) (2010) 421–431.
[25] J.Y. Zhang, F. Wang, H. Zhang, et al., Rapid identification of polymethoxylated flavonoids in traditional Chinese medicines with a practical strategy of stepwise mass defect filtering coupled to diagnostic product ions analysis based on a hybrid LTQ-Orbitrap mass spectrometer, Phytochem. Anal. 25 (5) (2014) 405–414.
[26] C.J. Lai, T. Tan, S.L. Zeng, et al., An integrated high resolution mass spectrometric data acquisition method for rapid screening of saponins in Panax notoginseng (Sanqi), J. Pharm. Biomed. Anal. 109 (2015) 184–191.
[27] H. Wang, C. Zhang, T. Zuo, et al., In-depth profiling, characterization, and comparison of the ginsenosides among three different parts (the root, stem leaf, and flower bud) of Panax quinquefolius L. by ultra-high performance liquid chromatography/quadrupole-Orbitrap mass spectrometry, Anal. Bioanal. Chem. 411 (29) (2019) 7817–7829.
[28] J. Wang, H. Kong, Z. Yuan, et al., A novel strategy to evaluate the quality of traditional Chinese medicine based on the correlation analysis of chemical fingerprint and biological effect, J. Pharm. Biomed. Anal. 83 (2013) 57–64.
[29] X. Liu, Q.G. Zhou, X.C. Zhu, et al., Screening for potential active components of fangji huangqi tang on the treatment of nephrotic syndrome by using integrated metabolomics based on "correlations between chemical and metabolic profiles", Front. Pharmacol. 10 (2019) 1261.
[30] Y. Tian-Wei, Z. Jie, L. Tao, et al., Infrared spectrum identification of Porcini pilus from different habitats based on principal component analysis and cluster analysis, Spectrosc. Spectr. Anal. (6) (2016) 1726–1730.
[31] J. He, X. Lu, T. Wei, et al., Asperuloside and asperulosidic acid exert an anti-inflammatory effect via suppression of the NF-κB and MAPK signaling pathways in LPS-induced RAW 264.7 macrophages, Int. J. Mol. Sci. 19 (2018) 2027.
[32] X. Zhao, J. Wei, M. Yang, Simultaneous analysis of iridoid glycosides and anthraquinones in Morinda officinalis using UPLC-QqQ-MS/MS and UPLC-Q/TOF-MS (E), Mol. 23 (5) (2018) 1070.
[33] N. Gampe, A. Darcsi, S. Lohner, S. Beni, L. Kursinszki, Characterization and identification of isoflavonoid glycosides in the root of Spiny restharrow (Ononis spinosa L.) by HPLC-QTOF-MS, HPLC-MS/MS and NMR, J. Pharm. Biomed. Anal. 123 (2016) 74–81.
[34] J.Q. Yu, X.W. Sun, Z.W. Wang, L. Fang, X. Wang, Alkaloids from Melodinus henryi with anti-inflammatory activity, J. Asian Nat. Prod. Res. 21 (2019) 820–825.
[35] A.M. Gil-Villa, A.M. Alvarez, M. Velásquez-Berrío, M. Rojas-López, P.C.J. Angela, Role of aspirin-triggered lipoxin A4, aspirin, and salicylic acid in the modulation of the oxidative and inflammatory responses induced by plasma from women with pre-eclampsia, Am. J. Reprod. Immunol. 83 (2020).
[36] Y. Li, L. Zhang, X. Wang, W. Wu, R. Qin, Effect of Syringic acid on antioxidant biomarkers and associated inflammatory markers in mice model of asthma, Drug Dev. Res. 80 (2019) 253–261.
[37] J. Serrano-Román, P. Nicasio-Torres, E. Hernández-Pérez, E. Jiménez-Ferrer, Elimination pharmacokinetics of sphaeralcic acid, tomentin and scopoletin mixture from a standardized fraction of Sphaeralcea angustifolia (Cav.) G. Don orally administered, J. Pharm. Biomed. Anal. 183 (2020), 113143.
[38] X. Xu, J. Chang, P. Wang, et al., Effect of chlorogenic acid on alleviating inflammation and apoptosis of IPEC-J2 cells induced by deoxyniyalenol, Ecotoxicol. Environ. Saf. 205 (2020), 111376.
[39] Y. Zhang, W. Pu, M. Bousquenaud, S. Cattin, C. Rüegg, Emodin inhibits inflammation, carcinogenesis, and cancer progression in the AOM/DSS model of colitis-associated intestinal tumorigenesis, Front. Oncol. 10 (2021), 564674.
[40] Z. Ding, Y. Dai, H. Hao, et al., Anti-inflammatory effects of scopoletin and underlying mechanisms, Pharm. Biol. 46 (2009) 854–860.
[41] S. Jamuna, K. Karthika, S. Paulsamy, et al., Confertin and scopoletin from leaf and root extracts of Hypochaeris radicata have anti-inflammatory and antioxidant activities, Ind. Crop. Prod. 70 (2015) 221–230.
[42] L. Xianyuan, Z. Wei, D. Yaqian, Z. Dan, T. Xueli, D. Zhanglu, L. Guanyi, T. Lan, L. Menghua, Anti-renal fibrosis effect of asperulosidic acid via TGF-beta1/smad2/smad3 and NF-kappaB signaling pathways in a rat model of unilateral ureteral obstruction, Phytomedicine 53 (2019) 274–285.
[43] S.J. Hwang, Y.W. Kim, Y. Park, et al., Anti-inflammatory effects of chlorogenic acid in lipopolysaccharide- stimulated RAW 264.7 cells, Inflamm. Res. 63 (1) (2014) 81–90.
[44] X. Zheng, Y. Cheng, Y. Chen, et al., Ferulic acid improves depressive-like behavior in prenatally-stressed offspring rats via anti-inflammatory activity and HPA Axis, Int. J. Mol. Sci. 20 (3) (2019) 493.
[45] D.H. Kim, B. Sung, Y.J. Kang, et al., Anti-inflammatory effects of betaine on AOM/DSS-induced colon tumorigenesis in ICR male mice, Int. J. Oncol. 45 (3) (2014) 1250–1256.
[46] R. Gautam, K.V. Karkhile, K.K. Bhutani, et al., Anti-inflammatory, cyclooxygenase (COX)-2, COX-1 inhibitory, and free radical scavenging effects of Rumex nepalensis, Planta Med. 76 (2010) 1564–1569.